Climate change and adaptive land management in southern Africa

Biodiversity & Ecology 6

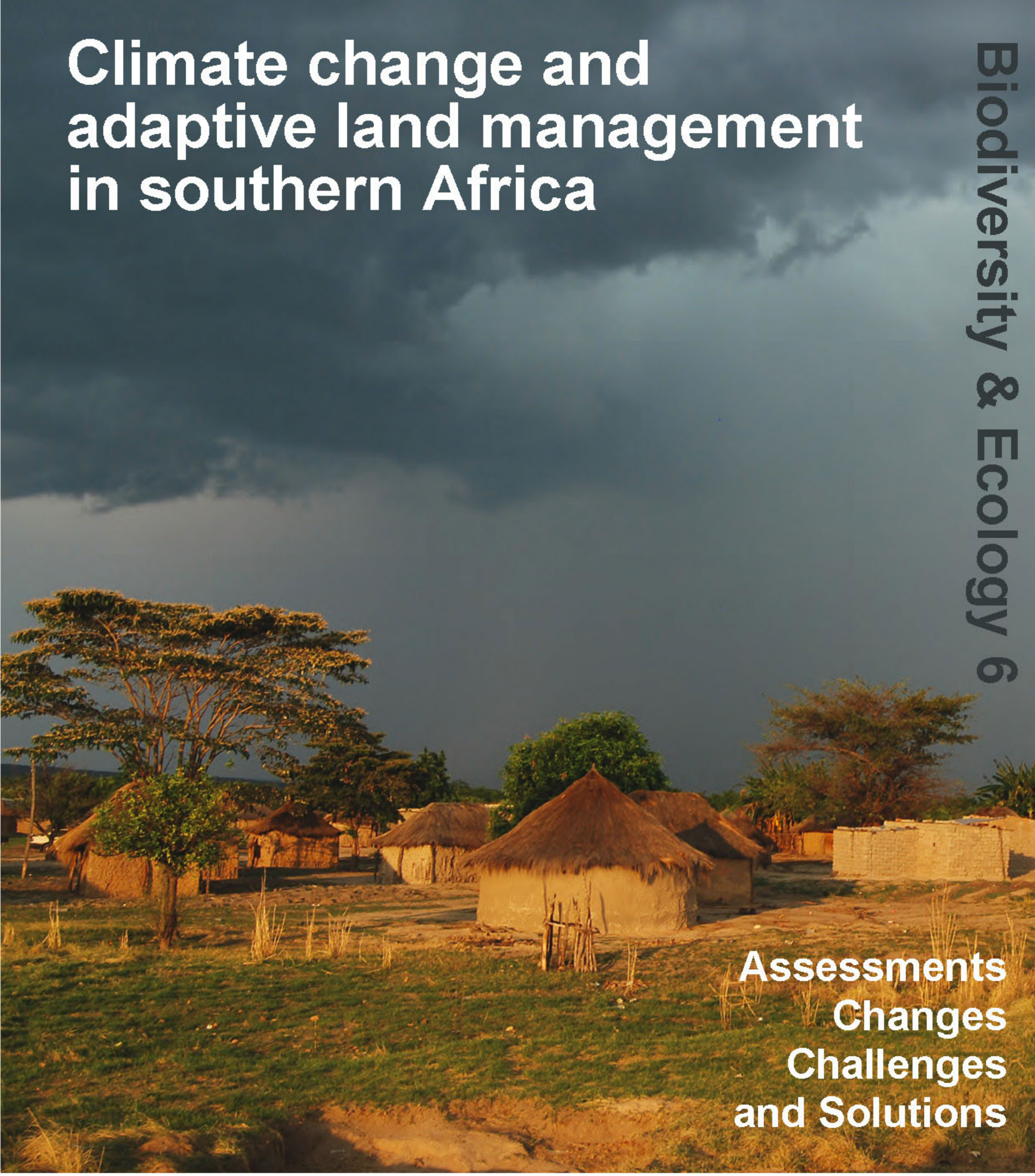

Assessments
Changes
Challenges
and Solutions

Product of the first research portfolio of

SASSCAL 2012–2018

Southern African
Science Service Centre for
Climate Change and
Adaptive Land Management

SPONSORED BY THE

Federal Ministry
of Education
and Research

Klaus Hess Publishers
Göttingen & Windhoek
www.k-hess-verlag.de

ISBN: 978-3-933117-95-3 (Germany), 978-99916-57-43-1 (Namibia)

Language editing: Will Simonson (Cambridge), and Proofreading Pal
Translation of abstracts to Portuguese: Ana Filipa Guerra Silva Gomes da Piedade
Page desing & layout: Marit Arnold, Klaus A. Hess, Ria Henning-Lohmann
Cover photographs:
front: Thunderstorm approaching a village on the Angolan Central Plateau (Rasmus Revermann)
back: Fire in the miombo woodlands, Zambia (David Parduhn)
Cover Design: Ria Henning-Lohmann

ISSN 1613-9801

Printed in Germany

Suggestion for citations:
Volume:
Revermann, R., Krewenka, K.M., Schmiedel, U., Olwoch, J.M., Helmschrot, J. & Jürgens, N. (eds.) (2018) Climate change and adaptive land management in southern Africa – assessments, changes, challenges, and solutions. *Biodiversity & Ecology*, **6**, Klaus Hess Publishers, Göttingen & Windhoek.

Articles (example):
Archer, E., Engelbrecht, F., Hänsler, A., Landman, W., Tadross, M. & Helmschrot, J. (2018) Seasonal prediction and regional climate projections for southern Africa. In: *Climate change and adaptive land management in southern Africa – assessments, changes, challenges, and solutions* (ed. by Revermann, R., Krewenka, K.M., Schmiedel, U., Olwoch, J.M., Helmschrot, J. & Jürgens, N.), pp. 14–21, *Biodiversity & Ecology*, **6**, Klaus Hess Publishers, Göttingen & Windhoek.

Corrections brought to our attention will be published at the following location:
http://www.biodiversity-plants.de/biodivers_ecol/biodivers_ecol.php

Biodiversity & Ecology

Journal of the Division Biodiversity, Evolution and Ecology of Plants,
Institute for Plant Science and Microbiology, University of Hamburg

Volume 6:

Climate change and adaptive land management in southern Africa

Assessments, changes, challenges, and solutions

Edited by

Rasmus Revermann[1], Kristin M. Krewenka[1], Ute Schmiedel[1],
Jane M. Olwoch[2], Jörg Helmschrot[2,3], Norbert Jürgens[1]

1 Institute for Plant Science and Microbiology, University of Hamburg
2 Southern African Science Service Centre for Climate Change and Adaptive Land Management
3 Department of Soil Science, Faculty of AgriSciences, Stellenbosch University

Hamburg 2018

Please cite the article as follows:

Röder; A., Stellmes, M., Frantz, D. & Hill, J. (2018) Remote sensing-based environmental assessment and monitoring – generation of operational baseline and enhanced experimental products in southern Africa. In: *Climate change and adaptive land management in southern Africa – assessments, changes, challenges, and solutions* (ed. by Revermann, R., Krewenka, K.M., Schmiedel, U., Olwoch, J.M., Helmschrot, J. & Jürgens, N.), pp. 344-354, *Biodiversity & Ecology*, **6**, Klaus Hess Publishers, Göttingen & Windhoek. doi:10.7809/b-e.00344

Land cover dynamics

Remote sensing-based environmental assessment and monitoring – generation of operational baseline and enhanced experimental products in southern Africa

Achim Röder[1]*, Marion Stellmes[1, 2], David Frantz[1,3], and Joachim Hill[1]

1 Department of Environmental Remote Sensing and Geoinformatics, Faculty of Regional and Environmental Sciences, Trier University, Behringstraße 15, 54286 Trier, Germany
2 Institute of Geographical Sciences, Remote Sensing and Geoinformatics, Department of Earth Sciences, Freie Universität Berlin, Malteserstraße 74–100, 12249 Berlin, Germany
3 Geomatics Lab, Geography Department, Humboldt-Universität zu Berlin, Unter den Linden 6, 10099 Berlin, Germany

* Corresponding author: roeder@uni-trier.de

Abstract: The spatial extension of the countries covered by SASSCAL, the diversity of their landscapes, and the range of social and ecological processes, constitute a challenge to environmental research. The latter have sometimes needed to focus on small test sites for very specific questions, or else required data and methods that allowed large area assessments. In either situation it is important that the studies are founded on consistent and comparable data. Responding to this requirement, a range of products based on operational earth observation satellite systems has been developed in the frame of SASSCAL. Here, we introduce the most relevant primary and derived products at coarse (250–500 m MODIS) and medium (30 m Landsat) spatial resolution, describe their basic properties, and provide examples of application as an impetus for further research. At the same time, alternative sources of data and advances in sensor systems offer high potential in complementing information from operational products, or provide further insights into specific local questions. We thus briefly touch upon the potential of such systems, including active sensing and/or airborne technologies such as Synthetic Aperture Radar, Light Detection and Ranging, use of Unmanned Aerial Vehicles (UAV), and hyperspectral imaging, and introduce studies carried under SASSCAL using these systems.

Resumo: A extensão espacial dos países envolvidos com o SASSCAL, a diversidade das suas paisagens e a variedade dos processos sociais e ecológicos constituem um desafio para a pesquisa ambiental. O último aspecto necessitou, por vezes, de se focar em pequenos locais de teste para questões muito específicas, ou requerer dados e métodos que permitiram avaliações de grandes áreas. Porém, em qualquer das situações, é importante que os estudos se baseiem numa base de dados consistente e comparável. Em resposta a este requisito, e no âmbito do SASSCAL, foi desenvolvida uma gama de produtos com base nos sistemas de satélite operacionais de observação da Terra. Aqui, introduzimos os produtos primários e derivados mais relevantes em resolução espacial grosseira (250 – 500 m MODIS) e média (30 m Landsat), descrevemos as suas propriedades básicas e oferecemos exemplos de aplicação como um incentivo para posterior investigação. Simultaneamente, fontes alternativas de dados e avanços nos sistemas de sensores oferecem um alto potencial na complementação da informação de produtos operacionais, ou fornecem uma visão mais aprofundada sobre questões locais específicas. Assim, abordamos resumidamente o potencial de tais sistemas, incluindo tecnologias de detecção activa e/ou sistemas aéreos, tais como Radar de Abertura Sintética, tecnologia LIDAR (Light Detection and Ranging), Veículos Aéreos Não Tripulados (UAV) e sistemas de imagens hiperespectrais, e introduzimos estudos desenvolvidos no âmbito do SASSCAL que utilizaram estes sistemas.

Introduction

In the face of climate change and imminent transformation processes, the need to evaluate state indicators of social-ecological systems or monitor their development is more pressing than ever (Scholes et al., 2008; Verstraete et al., 2011). Aside from specifically tailored case studies, many questions can only be tackled at regional, national or even continental scales (e.g. reporting for the "Reducing Emissions from Deforestation and Forest Degradation" programme of the UNFCCC, Herold et al. (2011a)), thus requiring adequate datasets. Recent advances in sensor technology allow the derivation of more sophisticated environmental indicators than ever before. Whilst such approaches have been possible in recent years, they have often been limited to specific locations due to data costs or the need to employ experimental sensors.

On the other hand, and despite their limitations in terms of spectral, geometric and radiometric properties, the existence of freely accessible long-term remote sensing archives, such as those of NOAA-AVHRR, Landsat or MODIS, allows the tracking of environmental processes back to the early 1970s and across large areas. Recently Hansen et al. (2013) have provided a global estimation of deforestation between 2000 and 2013 based on Landsat imagery, and DeFries et al. (2007) have suggested a multi-scale framework for estimating greenhouse gas emissions from deforestation based on different sensor systems. In many cases, global, ready-to-use earth observation products are not adequate for specific research tasks such as time series or spectral analyses, and particular requirements emerge in terms of quantitative consistency standards and data pre-processing. For instance, applying advanced quantitative interpretation or classification techniques to sequences of optical data (e.g. Landsat or Sentinel-2) often requires these to be quantitatively consistent, necessitating correction of atmospheric effects, variations in sun position, influences of topography, etc. In the context of data with high temporal resolution (e.g. 16- or 8-day composite MODIS data), often only base products (reflectance, vegetation indices) often exist, while more ecologically meaningful data representing seasonal dynamics within and across years need to be specifically derived. Given the amount of data that can potentially be used, procuring pre-processed datasets for subsequent analyses poses considerable demands in terms of data volumes and processing capabilities.

Many applied users are interested in earth observation data but have no mandate or capability to deal with extensive data pre-processing strategies. For this reason, operational data processing frameworks may facilitate the use of satellite data in many fields. One example is the framework for optical remote sensing processing (Framework for Operational Radiometric Correction for Environmental monitoring, FORCE) that has been implemented to prepare data products at different processing levels. These may be utilised in a variety of applications and in response to requirements of different levels of users, ranging from large-area classification of land-use and land-cover units, to the detailed analysis of deforestation or forest degradation in a regional context.

In many cases, such products might be complemented by additional information derived from other sources. First and foremost, active systems like Synthetic Aperture Radar (SAR) is of interest here, with various spaceborne platforms having been launched in recent years, including Terra-SAR and Sentinel-1. ESA's Sentinel-1 fleet is the first SAR system to operationally provide global data at high spatial resolution of 10 by 10 m at no cost to the user. Numerous studies have demonstrated the potential of using radar data as standalone or in combination with optical data (Joshi et al., 2016). For instance, Reiche et al. (2015) have demonstrated the potential of improving Landsat-based NDVI time series with ALOS-PALSAR data to compensate for cloudiness and improve time series analysis. Likewise, Stefanski et al. (2014) combined Landsat-TM and ERS2-SAR data to significantly increase mapping accuracies of land management regimes in western Ukraine.

Besides spaceborne sensors, airborne systems offer unique potential in enhancing operational products or supplying specific datasets for local applications, for instance to provide biophysical and structural information on vegetation communities at plot level. Airborne single pulse or full waveform Light Detection and Ranging (LiDAR) systems have gained increasing attention for ecological studies (Lefsky et al., 2002) and in recent years there has been a growing number of studies of savanna systems (Lucas et al., 2011). Armston et al. (2013) directly retrieved canopy gap fraction from waveform LiDAR, while Lucas et al. (2006) demonstrated the use of local-scale airborne LiDAR data to calibrate radar-based biomass models of forest systems for larger areas. Airborne hyperspectral data are another valuable source of information, recording optical reflectance information in often more than 100 spectral bands. While such data may serve to map floristic patterns (Oldeland et al., 2010), their integration with active systems is particularly promising. Naidoo et al. (2012), Cho et al. (2012) and Colgan et al. (2012) presented different approaches of combining hyperspectral and LiDAR data to classify savanna tree species. Finally, Unmanned Aerial Vehicles (UAV) provide additional flexibility in data acquisition, since they can be operated at short notice without the need to organise fully-fledged flight campaigns. At the same time an increasing array of sensor systems from multi-spectral to hyperspectral and LiDAR sensors have become available (Colomina & Molina, 2104), and even simple multi-spectral systems that include near-infrared imaging capabilities can be useful in discriminating woody species in savanna systems (Oldeland et al., 2017).

Our paper describes the different operational remote sensing processing modules developed in the context of the SASSCAL initiative, introduces the derived products and refers to example applications. Further studies using active and experimental sensors carried out in the frame of the SASSCAL initiative are also described.

Methods

Coarse resolution products

The MODIS platforms Terra and Aqua have acquired earth observation data since the year 2000 and 2002 respectively, providing imagery of the entire globe within 1 to 2 days with a spatial resolution of 250 by 250 m to 1 by 1 km, depending on the spectral band. The spectral specifications of the MODIS sensors allow for the derivation of numerous products for monitoring land, oceans and the atmosphere. The land related products are mainly distributed by "The Land Processes Distributed Active Archive Center" (LP DAAC) within the NASA Earth Observing System Data and Information System (EOSDIS). Within SASSCAL, we were specifically interested in providing information on land cover characteristics as well as the fire regime covering the whole of southern Africa, comprising the countries Angola, Zambia, Namibia, Botswana, and South Africa.

Phenology metrics

Information on phenology is an important indicator for the characterisation of the status and dynamics of land use/cover (Andres et al., 1994). It can be reliably mapped from many earth observation systems, and is commonly associated with photosynthetic activity (or "greenness") of vegetation. If such information is to be used for monitoring land cover dynamics, preferably long time periods need to be covered (Stellmes et al., 2013b). This information can be spatially provided by earth observation data with a high temporal repetition rate as acquired from sensors such as MODIS, SPOT-VEGETATION or NOAA-AVHRR.

To capture the land surface phenology (LSP) of the study region we used the 16-day Vegetation Indices (VI) Dataset at 250 m spatial resolution (Huete et al., 1999). It comprises different information layers, which are compiled from daily observations on a pixel basis from the best suitable information for the respective 16-day period. These layers include spectral vegetation indices (such as NDVI or EVI), reflectance values in different bands, and different auxiliary data on image acquisition conditions (e.g. viewing angles and observation quality). Importantly, for every pixel the exact date from which the data originated is recorded. The complete time series of the Terra and the Aqua MODIS sensors (MOD13Q1 and MYD13Q1 products, respectively) was incorporated for the period from 2000/2001 to 2012/2013. We used the Enhanced Vegetation Index (EVI) as a robust proxy for biomass development that reduces the impact of atmospheric influences and decouples the vegetation canopy signal from its background (i.e. soil and bedrock) signal based on reflectance in the blue, red and near-infrared bands. The day-of-composite information (i.e. the exact day from which a pixel in the composite originates) was used as the time axis and the Usefulness Index (Huete et al., 1999), an indication of the respective pixel's assumed quality (considering aerosol quantity, atmospheric correction conditions, cloud cover, shadow and sun-target-viewing geometry) was used to weight the data points during the fitting procedure.

Figure 1: Three years of a MODIS Enhanced Vegetation Index (EVI) time series (thin line) and fitted smooth B-spline (thick line) (from Mader (2012); further information in the text).

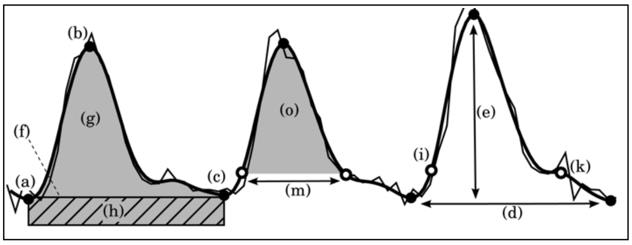

Table 1: Overview of parameters derived using the spline algorithm.

Index	Description	Ecological meaning
a	Day of year (DOY) and modelled value for early minimum of season (MOS)	Minimum greenness at beginning of the vegetation cycle and its day of occurrence
b	DOY and modelled value for peak of season (POS)	Maximum greenness within the vegetation cycle and its day of occurrence
c	DOY and modelled value for late minimum of season (MOS)	Minimum greenness at end of vegetation cycle and its day of occurrence
d	Duration (days) between successive minima	Length of vegetation cycle
e	Amplitude of Enhanced Vegetation Index (EVI) value as difference between peak and latent value (f)	Measure of the strength of the annual variability of greenness
f	Latent EVI value as average of the early and late minimum values	Measure related to the standing biomass
g	Integral between two successive minima	Measure related to the variable biomass
h	Latent integral	Measure related to the standing (invariant) biomass
g+h	Total integral defined as the sum of g and h	Measure related to the overall biomass within a vegetation cycle
i	Beginning (day of year) of greenness and modelled value for start of greenness	Metric related to the start of the vegetation period linked to a percent change in greenness and its day of occurrence
k	End (day of year) of greenness and modelled value for end of greenness	Metric related to the end of the vegetation period linked to a percent change in greenness and its day of occurrence
m	Duration of greenness defined as time span in days between i and k	Metric related to the length of the vegetation period as defined by the beginning and end of the vegetation period
o	Greenness integral defined by i and k	Metric related to the overall greenness/biomass generated within the vegetation period
	Rate of green-up defined as the slope of a line connecting the point of the onset of greenness and the annual peak value (not shown in Figure 1)	Metric related to the rate of greening up
	Rate of senescence, which is the (absolute) slope of the line connecting the annual peak and the point of end of greenness (not shown in Figure 1)	Metric related to the rate of senescence

MODIS LSP metrics were obtained by applying the Spline analysis of Time Series (SpliTS) algorithm (Mader, 2012). SpliTS is a C++ computer code for fitting spline models to remotely-sensed time series and to derive land surface phenology. It is a data-driven method that can handle non-equidistant time series considering the actual acquisition date. A set of 20 metrics is derived for each pixel, including date-specific parameters, and integral information about the growing seasons, amplitudes, etc., as illustrated in Figure 1 and summarised in Table 1.

Fire-related products

Changing boundary conditions, for example decreasing rainfall and/or land-use change related to population growth, may have major implications for the fire regime and in consequence for ecosystem functioning. Therefore, it is crucial to understand and describe all components of the prevailing fire regime. The key parameters that describe a fire regime are fire type, frequency, seasonality, intensity (largely determined by fuel load), spread and heat yield (Graz, 2003; Keeley, 2009).

We characterised the fire regime based on an extensive multi-scale compilation of the MODIS products "Active Fire" (AF) and "Burned Area" (BA) covering the period 2000 to 2015 and providing data with a spatial resolution of 1 km and 500 m, respectively. Based on the methodology proposed by Stellmes et al. (2013e), the integrated analysis of these mutually exclusive datasets allowed for a comprehensive spatio-temporal characterisation of important descriptors of the large-scale fire regime such as the fire frequency, seasonality and intensity, among others.

Moreover, we developed a novel object-based methodology that extracts valuable information about fire dynamics from BA data for every single fire detected and provides highly valuable information about fire dynamics that have not been spatially available up to now (Frantz et al., 2016e). Based on image segmentation of BA data and the analysis of movement trajectories between dates, detailed information for every single fire regarding timing and location of its ignition is recorded, as well as detailed directional multi-temporal spread information (i.e. the movement direction of the fire front and its speed). This information can in turn be integrated to derive large-scale information for the entire study area and to improve understanding of the overall fire regime.

Medium resolution products

Getting access to all recorded Landsat images, thanks to the opening of the archive (Woodcock et al., 2008), has provided unprecedented opportunities for long-term monitoring of a wide range of land surface indicators (Wulder et al., 2008; Danaher et al., 2010). In particular, it was possible to move from the analysis of a small set of images (Röder et al., 2008) to coverage of large areas (Griffiths et al., 2013a), and approaches utilising the full temporal depth of the Landsat archive (Kennedy et al., 2010). Yet, realising this potential poses challenges in terms of automated data pre-processing to ensure quantitative consistency of data.

Landsat archive pre-processing

We developed a pre-processing framework for Landsat imagery that incorporates the specific characteristics of the Thematic Mapper, Enhanced Thematic Mapper and Operative Land Imager sensors and adopts a tiling structure independent of the frames downloaded from Landsat's World Reference System (WRS-2) (Frantz et al., 2016a). We download all L1T images with less than 70% cloud cover. This processing level includes radiometric calibration and ground control point-based orthorectification including a digital elevation model to account for relief displacement. Subsequently, a modified version of the FMask algorithm (Zhu & Woodcock, 2012) is utilised to detect clouds and cloud shadows for every image. It has been modified for enhanced performance in savanna ecosystems with their co-occurrence of surfaces of largely different colour and surface temperature (Frantz et al., 2015a). The core of the processing chain is based upon the formulation of the radiative transfer initially introduced by Tanré et al. (1990), which considers the impact of gases and aerosols on absorption, direct and diffuse scattering, the sun-sensor-surface configuration and environmental effects, and models these processes. To facilitate operational implementation, the algorithm is parameterised with consideration of aerosol optical thickness and water vapour transmission factors. The latter are derived from concurrent MODIS water vapour data (MOD05 and MYD05 products, MOD03 and MYD03 geolocation tables), or a fallback model based on seasonal date and location for Landsat images acquired prior to the MODIS era or where no appropriate MODIS dataset is available. Aerosol optical depth (AOD) is estimated over dark targets, making use of a precompiled dark object database. This holds pixels that have been identified as persistent dark features in a first iteration of all available images. Again, a fallback model based on seasonal date and location is employed where an image-based estimation is not possible. As an advancement over most large-area data production systems, a modified C-based topography-correction is included in the radiative transfer model, where the C factor is derived from a slope- and surface-class-specific linear regression between the cosine of the illumination angle and the spectral radiance from an inclined surface. As a further important element, a correction of bidirectional effects using global parameters supplied by (Roy et al., 2016) was implemented.

Finally, the resulting dataset is projected to tiles of 1000 x 1000 pixels (or 30 km x 30 km) using bilinear resampling and second-order polynomial warping to a Lambert azimuthal equal area projection centred at the KAZA Transfrontier Conservation Area. For technical details of any processing step, refer to Frantz et al. (Frantz et al., 2015c; Frantz et al., 2015a; Frantz et al., 2016a).

Phenology fusion

As has already been outlined in the Methods section of this chapter, satellite-derived land surface phenology (LSP) is an important source of information and may be utilised both to stratify further analyses and to serve as an important input component for land cover mapping, change detection and other processes (Stellmes et al., 2013b). The derivation of phenology metrics is most commonly based on images with a high temporal resolution, such as NOAA-AVHRR or MODIS, and using a range of methods, such as Fourier transform, wavelet transform or spline fitting (Jonsson & Eklundh, 2002). As a result, phenological metrics may be derived representing the long-term average situation or at yearly intervals, the latter also supporting time series analysis of phenological indicators (Stellmes et al., 2013b). Although many applications would benefit from the existence of phenology at higher resolutions (e.g. 30 m x 30 m corresponding to Landsat pixel size) their derivation is often complicated by limitations in data availability, which is particularly relevant in regions with distinct dry/wet season periods, such as those in many south-African countries. This shortcoming could be overcome by implementing image fusion algorithms such as StarFM (Gao et al., 2006) to simulate images with high spatial and temporal resolution, and use these to derive phenology metrics. However, this entails a massive overhead in terms of processing efforts and capacities required and may still not be feasible due to lack of sufficient image density (in particular during the wet season) and high landscape heterogeneity, which has been shown to reduce fusion quality. To overcome this, we have developed a method (*ImproPhe*) to predict selected phenology parameters at medium (Landsat) resolution (MR) directly from coarse resolution (CR) phenology (outlined in the Methods section). The method is based on the assumption that a few MR temporal observations are sufficient to separate image regions with similar phenology directly and to high precision, even if their temporal resolution would not allow the derivation of land surface phenology descriptors in a classic procedure (Frantz et al., 2016g). Accordingly, we relate the accurate CR LSP to the corresponding MR spatial features by exploiting their spatio-temporal patterns, which is similar to the StarFM approach (Gao et al., 2006). We define several proxies at both resolutions that define the final neighbouring pixel's weight. These proxies include the spectral distance, the heterogeneity of the MR pixels and the heterogeneity of CR pixels within the analysis window. To account for different units and ranges of input data and to increase the contrast between the best and worst weights, the retrieved neighbour weights are rescaled through a sigmoidal transfer function (Frantz et al., 2016g).

Phenology-adaptive image compositing

Considering the scale of many urgent environmental questions, and the need to cover large areas to meet reporting requirements such as those of the REDD+ programme (Herold et al., 2011b), specific challenges emerge concerning the appropriate input satellite products. In particular, cloud cover and processing capabilities may be obstacles to such large-area, wall-to-wall applications. With the availability of large data archives, mosaicking and compositing methods have emerged that can help to mitigate both constraints. While mosaicking commonly joins individual images, compositing is carried out at the pixel level. Numerous techniques have been developed, which are often based on the optimisation of band or index statistics (Flood et al., 2013) and aim at providing regularly spaced time series. Where adverse climatic settings and non-systematic acquisition plans prevent gap-free annual coverage, compositing approaches may consider observations from various years, which have first been combined with additional spectral criteria in a parametric weighting scheme by Griffiths et al. (2013b). One key aspect in such compositing schemes is the treatise of phenology, since the same type of vegetation community may be in different growing stages at one acquisition date due to different local climatic conditions. We therefore made use of the processed Landsat archive (outlined in the Methods section) and the phenology fusion approach (outlined in the Methods section) to develop a parametric weighting scheme that allows the generation of pixel-based, phenology-adaptive composites of Landsat surface reflectance data, i.e. the creation of "synthetic" images with pixels assembled from a large body of satellite images (Frantz et al., 2017). This technique employs a parametric weighting scheme with full consideration of annual land surface phenology (LSP) at the pixel scale to generate phenologically coherent composites. The technique may be applied to any gridded earth observation data archive and, in general, six metrics are used to evaluate the suitability of each pixel in the archive.

The target acquisition day (Day of Year, DOY) is based on phenology metrics and calculated for each pixel based on the target phenological state. Peak of Season (POS), End of Season (EOS), and Minimum of Season (MOS) are used to fit Gaussian or logistic S-curves, from which the scoring function for the respective target season is derived.

For each composite, a target year for the compositing is set. Since it is often not possible to find a phenologically suitable pixel in that particular year, a number of bracketing years are defined, and an additional factor accounts for the trade-off between phenologically suitable date and target year to yield the respective scoring value. The cloud distance score makes use of the cloud and cloud shadow mask resulting from the pre-processing scheme, and devaluates pixels that are potentially affected. In addition, the Haze Optimised Transformation (HOT, Zhu & Woodcock 2012) is additionally used as input to account for potential haze contamination of pixels that were not flagged as cloud or cloud shadow. A correlation score is introduced that evaluates the stability of a given pixel by relating it to its spectral behaviour over time, thus minimising the impact of noise in the data and efficiently preventing artefacts from being considered for the compositing. Finally, a view angle score is defined to favour near nadir observations to those at larger view angles. These scores are then calculated for every candidate pixel and at every position in the desired compositing region to identify the most suitable pixel.

In addition to the actual reflectance composite, a number of compositing metrics are computed that provide further information about the composite and can be used directly for different applications. These metrics include spectral average, standard deviation, kurtosis and skewness. Layers for each individual score and the overall score of the finally selected pixel are also generated (Frantz et al., 2017).

Results

Modis

Overall, 20 phenology metrics were derived for southern Africa on an annual basis (due to the growing season of the southern hemisphere starting in July) covering the period from 2000/2001 to 2012/2013.

Figure 2 depicts four phenological metrics that were derived for the SASSCAL countries. These are the means of: (i) the total integral, which can be related to the overall biomass; (ii) the latent integral associated with the standing biomass; (iii) the green integral, which is linked to the variable biomass within the vegetation period; and (iv) the day of year (DOY) of the start of greening. All metrics show that the study area is characterised by strong phenological gradients that can be related to the major functional vegetation types, to a large degree determined by climatological gradients. Whereas the subtropical Miombo belt in Angola and Zambia is characterised by a high total and latent integral, the Namib, which typifies the dry extreme of the study

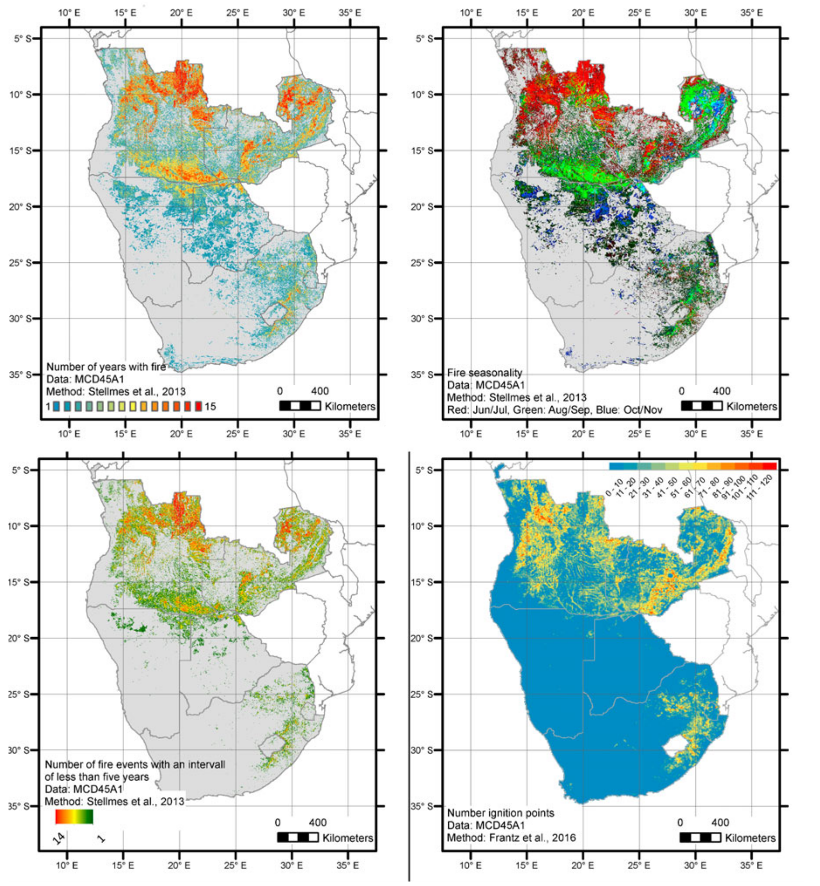

Figure 2: Remotely-sensed characterisation of the fire regimes of southern Africa. Number of years with fire (upper left), fire seasonality (upper right), number of fire events with an interval of less than five years (lower left) and number of ignition points within the period 2000 to 2015 (lower right).

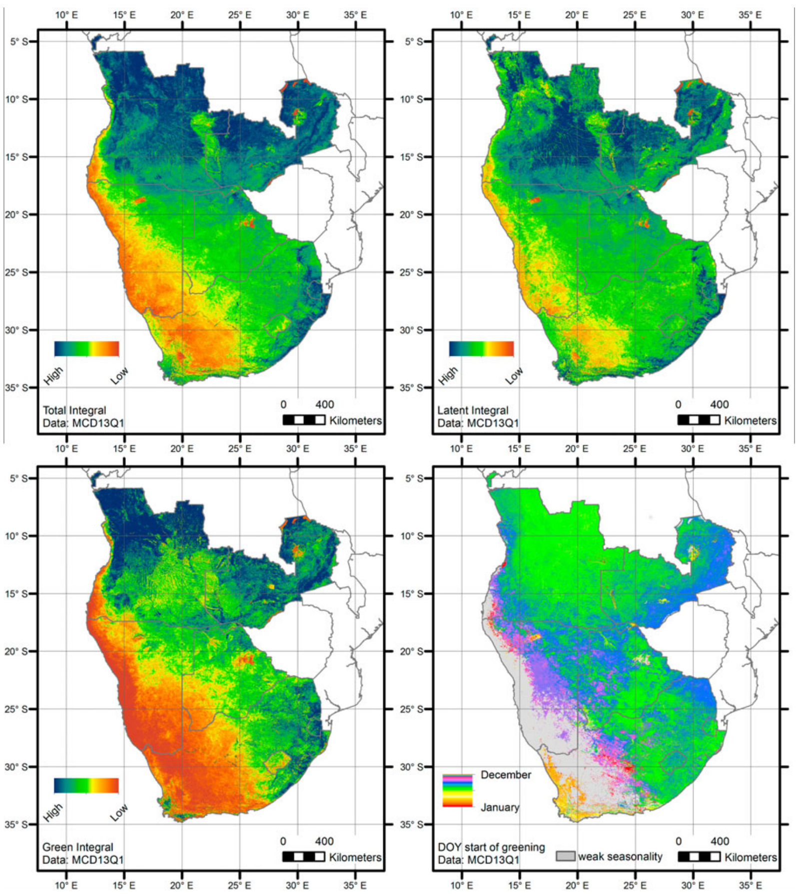

Figure 3: Mean total integral corresponding to total biomass (upper left), mean latent integral corresponding to standing biomass (upper right), mean green integral corresponding to variable biomass during the growing season (lower left) and day of year (DOY) of the start of greening for the observation period 2000/2001 to 2012/2013 (lower right).

area, is characterised by overall low vegetation cover. The phenology metrics are therefore capable of identifying the major functional vegetation types (Stellmes et al., 2013e) and might furthermore be utilised for large-area monitoring of land cover dynamics as well as for establishing relationships to climatic and anthropogenic drivers.

Fire related parameters

Based on the methodologies of Stellmes et al. (2013e) and Frantz et al. (2016e) a variety of fire regime related parameters were derived for the period covering 2000 to 2015. These parameters comprise established variables such as fire frequency, seasonality and intensity but also enhanced parameters such as the localisation of fire ignition points and fire spread rate. Figure 3 illustrates the capability of the used methodologies to provide important fire related information. The examples reveal the diversity of the fire regimes prevalent in the SASSCAL area, where fire frequency is high in grassland dominated ecosystems. These areas are therefore also characterised by high fire return intervals that are often too short to allow for the establishment of tree saplings. The fire seasonality is, in general terms, mainly characterised by a north—south gradient from early fires in June/July in northern Angola (red colour, Fig. 3) to later fires in the southern part (green and blue colours) that are often related to higher fire intensities.

Landsat

Landsat archive pre-processing

Covering the countries of Angola, Botswana, Namibia, Zambia, and Zimbabwe, we processed a total of 57,371 L1T images covering the period from 1984 to 2014, which corresponds to a surface area of 3.7 M km^2, 194 Landsat WRS-2 frames, 4524 tiles, 1,912,733 tiled datasets, and a total size of ~28 TB (Figure 4).

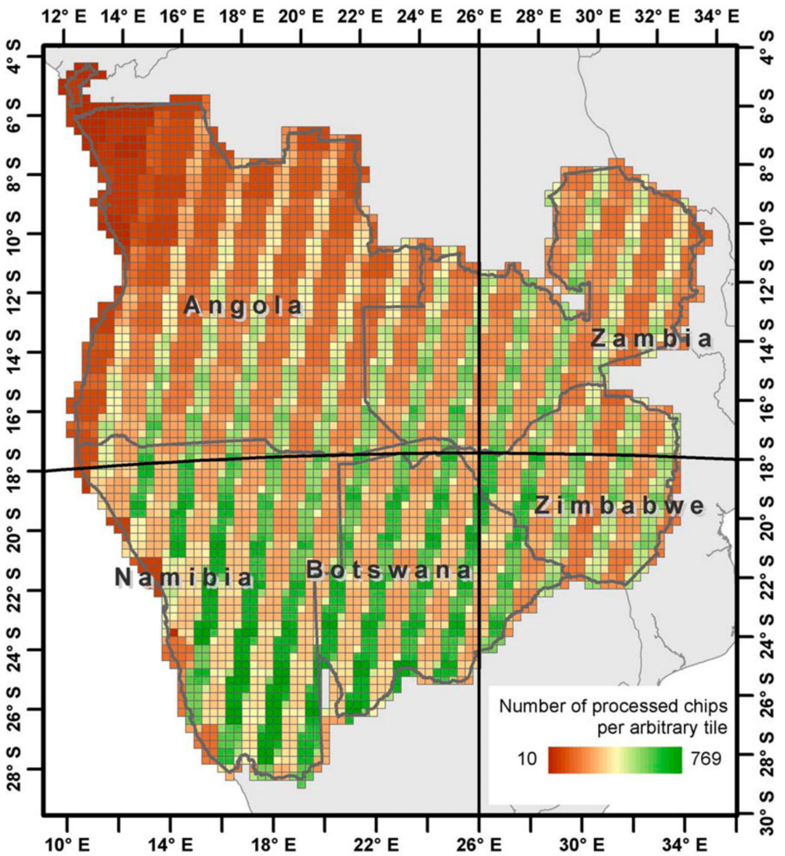

Figure 4: Number of processed Landsat images per tile. Redundant overlaps from the same path are excluded, whilst overlaps from neighbouring paths are visible as a striping pattern.

Since it is not feasible to carry out ground-based validation of reflectance values derived from large-area processing frameworks, we evaluated the spectral consistency of the results by making use of the along-path (i.e. consecutive rows) and across-path (i.e. neighbouring paths) overlap regions resulting from the image acquisition paths of Landsat data. We observed variations in the order of ±2.5% reflectance for 98.9% of all redundant image pairs. Furthermore, retrieved AOD estimates were compared with Aeronet stations located inside our project area with high coefficients of determination for all covered bands of the visible and near-infrared region. Uncertainty of water vapour absorption was assessed, and the robustness of the approach confirmed, through a sensitivity study over the Etosha pan, comparing values derived from the water vapour database with those derived from the MODIS products (Frantz et al. 2016a, b). The performance of the topography correction was evaluated by a relative analysis of NIR reflectance in different topographic aspect classes against a Minnaert-based correction and no correction, and our approach generally outperformed the other options (Frantz et al., 2015c; Frantz et al., 2016a).

All resulting images are stored in the gridded structure described before, where every tile contains all corrected reflectance images and the corresponding distances to the next cloud and cloud shadow. The structure is organised for easy data access, such that secondary indicators (e.g. vegetation indices) can be quickly calculated and stored as additional layers for further analysis.

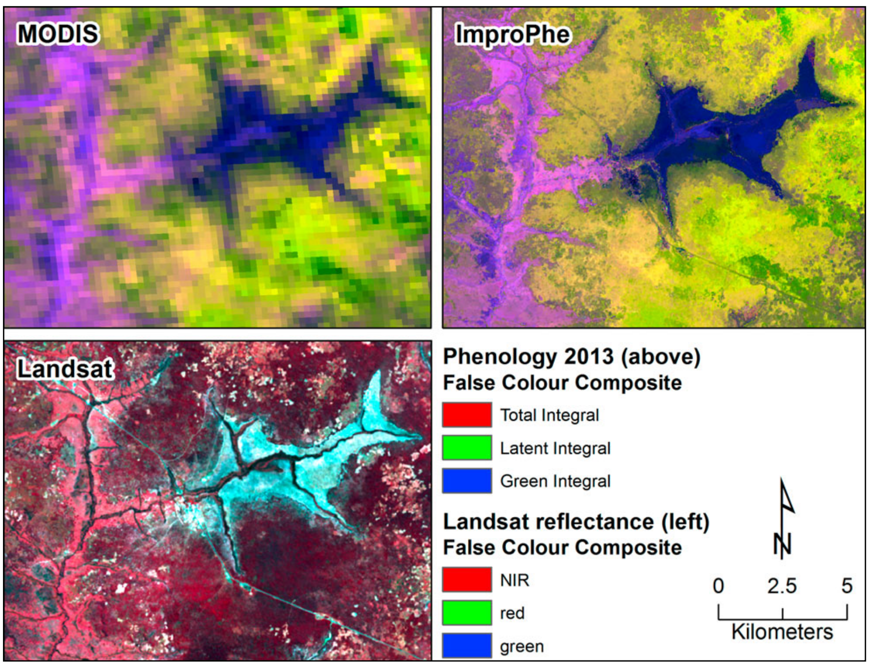

Figure 5: False colour composites of the Total Integral, Latent Integral and Green Integral in 2013. MODIS (above left), fusion result using the Improphe code (above right), and Landsat-8 image from May 2013 (below left).

Phenology fusion

We used MODIS-scale phenology as described before to parameterise the fusion algorithm. We evaluated the validity of our approach through a sensitivity study based on simulated data, which confirmed the performance of the different kernel-derived metrics (Frantz et al., 2016g). We then predicted the POS, EOS, MOS, and SOS (Start of Season) parameters for the 12-year period from 2001 to 2012 at Landsat spatial resolution for the entire study area and with a kernel size of 200 pixels. Figure 5 displays the prediction results as well as the input from the CR LSP.

Figure 5 shows the area around the city of Mumbué (Angola) characterised by the typical landscape elements in the study area. Whereas the valleys are dominated by grasslands, the summits are covered by dense Miombo forests, which are cleared for shifting cultivation purposes. The fused dataset substantially refines the spatial resolution of the LSP metrics and allows the better delineation of the land cover classes of the heterogeneous area compared to the MODIS LSP, while avoiding problems caused by data gaps when deriving LSP directly from Landsat time series. The grasslands are characterised by a high seasonal biomass (violet colour), the Miombo forests by high standing biomass (yellowish colour), whilst vegetation free areas show as dark blue colours. Arable land is quite diverse depending on whether the fields are in use or abandoned, but biomass amounts tend to be rather low compared to the natural vegetation cover. In general, object boundaries are well defined as shown in the agricultural areas, and even features that are barely discernible in the CR data, if at all, were reconstructed. Consequently, it is possible to predict at MR any phenological predictor existing at CR. The prediction quality is strongly dependent on the size of the analysis kernel, so the trade-off with processing time needs to be considered.

Phenology-adaptive image compositing

We calculated different seasonal composites for varying target dates and years. Where no distinct yearly phenological cycles could be calculated (i.e. in the pre-MODIS era), a long-term average phenology was used instead. Figure 6 depicts a composite showing the countries of Angola, Botswana, Namibia, Zambia, and Zimbabwe.

The image shown here is a cloud-free, seamless Landsat representation of the full area with a composite size of 91000 x 82000 pixels and a total image size of approximately 80 GB. Roughly 208 M observations (i.e. pixels) were considered in the procedure; for ease of data handling, composites are commonly produced for smaller areas.

While cross-comparisons with composites derived from MODIS reflectance data underline the robustness of the approach, reduced data availability between the termination of Landsat-5 and the operational phase of Landsat-8, as well as enhanced cloudiness during the wet season, affect the quality of the composites produced, with SLC-off patterns related to Landsat-7 ETM+ being visible particularly in POS-composites. In general, the large difference between selecting individually tailored DOYs for each pixel, as opposed to defining a general DOY, was confirmed by evaluating the effect along altitudinal gradients. Consequently, selection of dynamic or static parameterisation of phenology in the compositing procedure requires careful consideration of the intended task. For instance, static parameterisation might be beneficial for crop type discrimination (Van Niel & McVicar, 2004), and tree type identification in areas with altitudinal gradients are expected to benefit from the phenological de-phasing associated with a dynamic parameterisation (Stoffels et al., 2015).

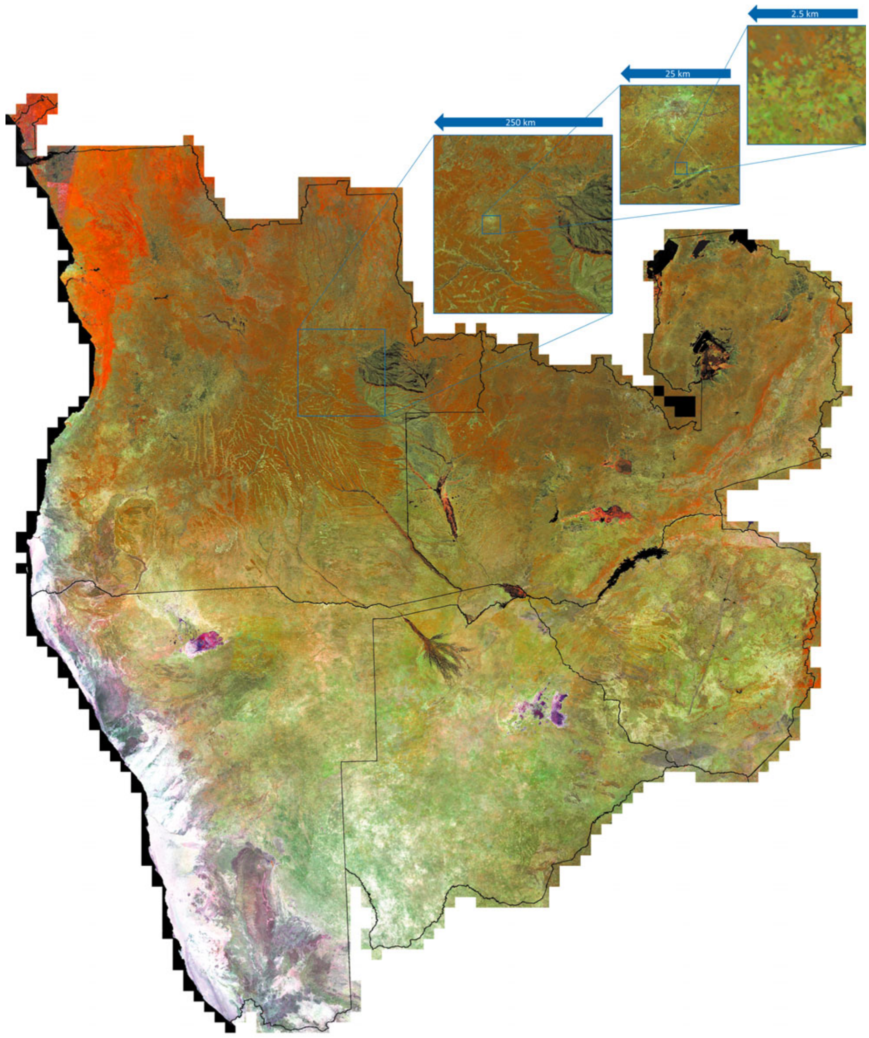

Figure 6: End-of-season composite of topography-corrected Landsat surface reflectance (RGB = Near Infrared – Short Wave Infrared – Red). Target year was 2008 ± 2 years.

Discussion

This chapter introduced the main remote sensing based primary and secondary geospatial products that were developed in the context of SASSCAL. With their unique geometric, spectral and temporal characteristics, they allow a variety of questions related to environmental monitoring and modelling to be addressed, either by using the primary (spectral) data, or by utilising the derived products such as fire metrics, phenology descriptors or reflectance composites.

For instance, Stellmes et al. (2013a) have employed the derived phenology metrics at coarse scale to provide a map of major vegetation types for the Okavango Basin, Udelhoven et al. (2015) have analysed the influence of rainfall on vegetation trends using distributed lag models, and Revermann et al. (2016) have successfully linked phenology information to a vegetation database to model floral diversity. The medium resolution Landsat database has been employed to analyse conversion dynamics in a cross-border study in northern Namibia and southern Angola using iterative spectral mixture analysis and support vector classification (Röder et al., 2015), and in different analyses in central Angola using temporal segmentation of time series derived indicators (e.g. Normalized Burn Ratio, NBR; Disturbance Index, DI). The latter studies have identified patterns of conversion to smallholder agriculture (Schneibel et al., 2016) and analysed subtle changes within forests to identify processes of forest degradation (Schneibel et al., 2018), for instance caused by selective logging or charcoal production, and to identify underlying causes of deforestation (Parduhn & Frantz, 2018). De Blécourt et al. (2018) evaluated land-use change processes in smallholder-dominated systems in Zambia and Angola based on multi-temporal Landsat datasets. Since fires are a major component in any of these systems and cause major effects in spectral image properties, the fire products are, besides their relevance in ecological studies, important explanatory factors to understand spatial patterns derived from satellite imagery.

The combined use of long-term archives of coarse and medium resolution satellite data offers unique opportunities to address questions ranging from locally-adapted, specific case studies, to wall-to-wall approaches required for national reporting. At present, new sensors are becoming available that may be used to complement the archives introduced here, such as the suite of Sentinel systems. Our radiometric processing scheme has already been successfully tested with Sentinel-2A data in central European environments, and incorporation of these data will further enhance temporal revisit capabilities. Ideally, the processing can be realised in near-real-time, thus paving the way for the implementation of short-term early warning systems (Zhu & Woodcock, 2014).

Complementing the development of an operational processing framework and utilisation of its products, different complementary studies and experimental case studies are presented in this book. Making synergetic use of ALOS/PALSAR radar data with a range of LiDAR flight transects, Mathieu et al. (2018) introduce a woody cover dataset for South Africa and highlight the potential of woody cover monitoring for different test areas in south-western Africa. Strohbach (2018) and Knox et al. (2018) demonstrate the potential of UAV imagery to map ecosystem characteristics in Namibian woodland and rangeland systems based on vegetation indices and derived three-dimensional features, respectively.

In summary, remote sensing techniques have successfully contributed to addressing a plethora of environmental and societal questions, ranging from large area, wall-to-wall assessments to local and regional case studies, and make use of the full range of observation systems available today.

These observation and mapping capabilities can be expected to expand further with the range of upcoming systems. Since February 2016, Sentinel-3A provides complementary information to the MODIS system while Sentinel-1 radar imagery may be able to supply additional perspectives not yet covered by optical systems, such that a long-term perspective for large-area monitoring is ensured. As such, different levels of detail may be addressed, with novel very high resolution systems commonly operated by commercial companies (e.g. the dove suite of sensors launched by Planet Inc. or the Worldview satellites by Digitalglobe Inc.) or sensors mounted on unmanned aerial vehicles (UAV) being able to supply the crucial element to link ground-observations to the large-area perspective.

Acknowledgements

The research was carried out in the framework of SASSCAL and was sponsored by the German Federal Ministry of Education and Research (BMBF) under promotion number 01LG1201C. We thank Dr. Sebastian Mader (Dept. of Environmental Remote Sensing and Geoinformatics, Trier University) for granting access to the SpliTS code. The National Aeronautics and Space Agency and the United States Geological Survey are acknowledged for providing Landsat and MODIS data. Two anonymous reviewers are thanked for providing valuable comments that greatly helped improve the manuscript. The FORCE processing framework is available for download from www.uni-trier.de/index.php?id=63673.

References

Andres, L., Salas, W.A. & Skole, D. (1994) Fourier analysis of multi-temporal AVHRR data applied to a land cover classification. *Journal of Remote Sensing*, **115**, 1115-1121.

Armston, J., Disney, M., Lewis, P.E., Scarth, P., Phinn, S., Lucas, R., Buntin, P. & Goodwin, N. (2013) Direct retrieval of canopy gap probaility using airborne waveform lidar. *Remote Sensing of Environment*, **134**, 24-38.

Cho, M.A., Mathieu, R., Asner, G.P., Naidoo, L., van Aardt, J., Ramoelo, A., Debba, P., Wessels, K., Main, R., Smit, I.P.J. & Erasmus, B. (2012) Mapping tree species composition in South African savannas using an integrated airborne spectral and LiDAR system. *Remote Sensing of Environment*, **125**, 214-226.

Colgan, M.S., Baldeck, C.A., Féret, J.-B. & Asner, G.P. (2012) Mapping Savanna Tree Species at Ecosystem Scales Using Support Vector Machine Classification and BRDF Correction Airborne Hyperspectral and LiDAR Data. *Remote Sensing*, **4**, 3462-3480.

Colomina, I. & Molina, P. (2104) Unmanned aerial systems for photogrammetry and remote sensing: A review. *ISPRS Journal of Photogrammetry and Remote Sensing*, **92**

Danaher, T., Scarth, P., Armston, J., Collett, L., Kitchen, J. & Gillingham, S. (2010) Remote Sensing of Tree-Grass Systems: The Eastern Australian Woodlands. *Ecosystem Function in Savannas: Measurement and Modeling at Landscape to Global Scales* (ed. by M.J. Hill and N.P. Hanan), pp. 175-194. CRC Press, Boca Raton, USA.

de Blécourt, M., Röder, A., Gröngröft, A., Baumann, S., Frantz, D. & Eschenbach, A. (2018) Deforestation for agricultural expansion in SW Zambia and NE Namibia and the impacts on soil fertility, and soil organic carbon and nutrient levels. This volume.

DeFries, R., Achard, F., Brown, S., Herold, M., Murdiyarso, D., Schlamadinger, B. & de Souza, C. (2007) Earth observations for estimating greenhouse gas emissions from deforestation in developing countries. *Environmental Science & Policy*, **10**, 385-394.

Flood, N., Danaher, T., Gill, T.K. & Gillingham, S.S. (2013) An Operational Scheme for Deriving Standardised Surface Reflectance from Landsat TM/ETM+ and SPOT HRG Imagery for Eastern Australia. *Remote Sensing*, **5**, 83-109.

Frantz, D., Röder, A., Udelhoven, T. & Schmidt, M. (2015a) Enhancing the Detectability of Clouds and Their Shadows in Multitemporal Dryland Landsat Imagery: Extending Fmask. *IEEE Geoscience and Remote Sensing Letters*, **12**, 1242-1246.

Frantz, D., Röder, A., Stellmes, M. & Hill, J. (2015c) On the Derivation of a Spatially Distributed Aerosol Climatology for its Incorporation in a Radiometric Landsat Preprocessing Framework. *Remote Sensing Letters*, **6**, 647-656.

Frantz, D., Röder, A., Stellmes, M. & Hill, J. (2016a) An Operational Radiometric Landsat Preprocessing Framework for Large-Area Time Series Applications. *IEEE Transactions on Geoscience and Remote Sensing*, **54**, 3928-3943.

Frantz, D., Stellmes, M., Röder, A. & Hill, J. (2016e) Fire spread from MODIS burned area data: obtaining fire dynamics information for every single fire. *International Journal of Wildland Fire*, -.

Frantz, D., Röder, A., Stellmes, M. & Hill, J. (2017) Phenology-adaptive pixel-based compositing using optical earth observation imagery. *Remote Sensing of Environment*, **190**, 331-347.

Frantz, D., Stellmes, M., Röder, A., Udelhoven, T., Mader, S. & Hill, J. (2016g) Improving the Spatial Resolution of Land Surface Phenology by Fusing Medium- and Coarse-Resolution Inputs. *IEEE Transactions on Geoscience and Remote Sensing*, **54**, 4153-4164.

Gao, F., Masek, J., Schwaller, M. & Hall, F. (2006) On the Blending of the Landsat and MODIS Surface Reflectance: Predicting Daily Landsat Surface Reflectance. *IEEE Transactions on Geoscience and Remote Sensing*, **44**, 2207-2218.

Graz, F.P. (2003) An HTML-based Concept Model of the Dry Savanna Woodland Ecosystem for Teaching and Learning. *Ecology & Society*, **7**, 9.

Griffiths, P., Müller, D., Kuemmerle, T. & Hostert, P. (2013a) Agricultural Land Change in the Carpathian Ecoregion after the Breakdown of Socialism and Expansion of the European Union. *Environmental Research Letters*, **8**

Griffiths, P., van der Linden, S., Kuemmerle, T. & Hostert, P. (2013b) A Pixel-Based Landsat Compositing Algorithm for Large Area Land Cover Mapping. *IEEE Journal of Selected Topics in Applied Earth Observations and Remote Sensing*, **6**, 2088-2101.

Hansen, M.C., Potapov, P.V., Moore, R., Hancher, M., Turubanova, S.A., Tyukavina, A., Thau, D., Stehman, S.V., Goetz, S.J., Loveland, T.R., Kommareddy, A., Egorov, A., Chini, L., Justice, C.O. & Townshend, J.R.G. (2013) High-Resolution Global Maps of 21st-Century Forest Cover Change. *Science*, **342**, 850-853.

Herold, M., Roman-Cuesta, R.M., Mollicone, D., Hirata, Y., Van Laake, P., Asner, G.P., Souza, C., Skutsch, M., Avitabile, V. & MacDicken, K. (2011a) Options for monitoring and estimating historical carbon emissions from forest degradation in the context of REDD#. *Carbon Balance and Management*, **6**, 1-7.

Herold, M., Román-Cuesta, R.M., Mollicone, D., Hirata, Y., Van Laake, P., Asner, G.P., Souza, C., Skutsch, M., Avitabile, V. & MacDicken, K. (2011b) Options for Monitoring and Estimating Historical Carbon Emissions from Forest Degradation in the Context of REDD+. *Carbon Balance and Management*, **6**, 1-7.

Huete, A., Justice, C.O. & Van Leeuwen, W. (1999) MODIS vegetation index (MOD13). *Algorithm theoretical basis document*, **3**

Jonsson, P. & Eklundh, L. (2002) Seasonality Extraction by Function Fitting to Time-Series of Satellite Sensor Data. *IEEE Transactions on Geoscience and Remote Sensing*, **40**, 1824-1832.

Joshi, N., Baumann, M., Ehammer, A., Fensholt, R., Grogan, K., Hostert, P., Jepsen, M.R., Kuemmerle, T., Meyfroidt, P., Mitchard, E.T.A., Reiche, J., Ryan, C.M. & Waske, B. (2016) A Review of the Application of Optical and Radar Remote Sensing Data Fusion to Land Use Mapping and Monitoring. *Remote Sensing*, **8**, 1-23.

Keeley, J.E. (2009) Fire intensity, fire severity and burn severity: a brief review and suggested usage. *International Journal of Wildland Fire*, **18**, 116-126.

Kennedy, R.E., Yang, Z. & Cohen, W.B. (2010) Detecting Trends in Forest Disturbance and Recovery using Yearly Landsat Time Series: 1. LandTrendr — Temporal Segmentation Algorithms. *Remote Sensing of Environment*, **114**, 2897-2910.

Lefsky, M.A., Cohen, W.B., Parker, G., G. & Harding, D.J. (2002) Lidar Remote Sensing for Ecosystem Studies. *BioScience*, **52**, 19-30.

Lucas, R., Cronin, N., Lee, A., Moghaddam, M., Witte, C. & Tickle, P. (2006) Empirical relationships between AIRSAR backscatter and LiDAR-derived forest biomass, Queensland, Australia. *Remote Sensing of Environment*, **100**, 407-425.

Lucas, R., Lee, A., Armston, J., Carreiras, J.M.B., Viergever, K.M., Bunting, P., Clewley, D., Moghaddam, M., Siqueira, P. & Woodhouse, I. (2011) Quantifying Carbon in Savannas: The Role of Active Sensors in Measurements of Tree Structure and Biomass. *Ecosystem Function in Savannas: Measurement and Modelling at Landscape to Global Scales* (ed. by M.J. Hill and N.P. Hanan), pp. 155-174. CRC Press, Boca Raton, London, New York.

Mader, S. (2012) *A Framework for the Phenological Analysis of Hypertemporal Remote Sensing Data Based on Polynomial Spline Models*. Ph.D. dissertation, Trier University, Trier, Germany.

Naidoo, L., Cho, M.A., Mathieu, R. & Asner, G.P. (2012) Classification of savanna tree species, in the Greater Kruger National Park region, by integrating hyperspectral and LiDAR data in a Random Forest data mining environment. *ISPRS Journal of Photogrammetry and Remote Sensing*, **69**, 167-179.

Oldeland, J., Große-Stoltenberg, A., Naftal, L. & Strohbach, B.J. (2017) The Potential of UAV Derived Image Features for Discriminating Savannah Tree Species. *The Roles of Remote Sensing in Nature Conservation. A Practical Guide and Case Studies.* (ed. by R. Diaz-Delgado, R. Lucas and C. Hurford), pp. 183-202. Springer, London, New York.

Oldeland, J., Dorigo, W., Lieckfeld, L., Lucieer, A. & Jürgens, N. (2010) Combining vegetation indices, constrained ordination and fuzzy classification for mapping semi-natural vegetation units from hyperspectral imager. *Remote Sensing of Environment*, **114**, 1155-1166.

Parduhn, D. & Frantz, D. (2018) "This is not Deforestation". Seeing deforestation in Zambia from afar and nearby. This volume.

Reiche, J., Verbesselt, J., Hoekman, D. & Herold, M. (2015) Fusing Landsat and SAR time series to detect deforestation in the tropics. *Remote Sensing of Environment*, **156**, 276-293.

Revermann, R., Finckh, M., Stellmes, M., Strohbach, B., Frantz, D. & Oldeland, J. (2016) Linking land surface phenology and vegetation-plot databases to model terrestrial plant alpha diversity of the Okavango Basin. *Remote Sensing*, **8**, 470.

Röder, A., Udelhoven, T., Hill, J., del Barrio, G. & Tsiourlis, G. (2008) Trend Analysis of Landsat-TM and -ETM+ Imagery to Monitor Grazing Impact in a Rangeland Ecosystem in Northern Greece. *Remote Sensing of Environment*, **112**, 2863-2875.

Röder, A., Pröpper, M., Stellmes, M., Schneibel, A. & Hill, J. (2015) Assessing urban growth and rural land use transformations in a cross-border situation in Northern Namibia and Southern Angola. *Land Use Policy*, **42**, 340-354.

Roy, D.P., Zhang, H.K., Ju, J., Gomez-Dans, J.L., Lewis, P.E., Schaaf, C.B., Sun, Q., Li, J., Huang, H. & Kovalskyy, V. (2016) A General Method to Normalize Landsat Reflectance Data to Nadir BRDF Adjusted Reflectance. *Remote Sensing of Environment*, **176**, 255-271.

Schneibel, A., Röder, A., Stellmes, M. & Frantz, D. (2018) Long-term lan use change analysis in south-central Angola. Assessing the trade-off between major ecosystem services with remote sensing data. This volume.

Schneibel, A., Stellmes, M., Röder, A., Finckh, M., Revermann, R., Frantz, D. & Hill, J. (2016) Evaluating the trade-off between food and timber resulting from the conversion of Miombo forests to agricultural land in Angola using multi-temporal Landsat data. *Science of the Total Environment*, **548**, 390-401.

Scholes, R.J., Mace, G.M., Turner, W., Geller, G.N., Jürgens, N., Larigauderie, A., Muchoney, D., Walther, B.A. & Mooney, H.A. (2008) Toward a Global Biodiversity Observing System. *Science*, **321**, 1044-1045.

Stefanski, J., Kuemmerle, T., Chaskovskyy, O., Griffiths, P., Havryluk, V., Knorn, J., Korol, N., Sieber, A. & Waske, B. (2014) Mapping Land Management Regimes in Western Ukraine Using Optical and SAR Data. *Remote Sensing*, **6**, 5279-5305.

Stellmes, M., Frantz, D., Finckh, M. & Revermann, R. (2013a) Okavango Basin - Earth Observation. *Environmental Assessments in the Okavango region* (ed. by J. Oldeland, C. Erb, M. Finckh and N. Jürgens), pp. 23-27.

Stellmes, M., Röder, A., Udelhoven, T. & Hill, J. (2013b) Mapping Syndromes of Land Change in Spain with Remote Sensing Time Series, Demographic and Climatic Data. *Land Use Policy*, **30**, 685-702.

Stellmes, M., Frantz, D., Finckh, M., Revermann, R., Röder, A. & Hill, J. (2013e) Fire frequency, fire seasonality and fire intensity within the Okavango region derived from MODIS fire products. *Biodiversity & Ecology*, **5**, 351-362.

Stoffels, J., Hill, J., Sachtleber, T., Mader, S., Buddenbaum, H., Stern, O., Langshausen, J., Dietz, J. & Ontrup, G. (2015) Satellite-Based Derivation of High-Resolution Forest Information Layers for Operational Forest Management. *Forests*, **6**, 1982-2013.

Tanré, D., Deroo, C., Duhaut, P., Herman, M., Morcrette, J.J., Perbos, J. & Deschamps, P.Y. (1990) Description of a Computer Code to Simulate the Satellite Signal in the Solar Spectrum: The 5S Code. *International Journal of Remote Sensing*, **11**, 659-668.

Udelhoven, T., Stellmes, M. & Röder, A. (2015) Assessing rainfall-EVI relationships in the Okavango catchment employing MODIS time series data and distributed lag models. *Remote Sensing Time Series. Revealing Land Surface Dynamics* (ed. by C. Kuenzer, S. Dech and S. Wagner), pp. 225-245. Springer, Berlin, Heidelberg.

Van Niel, T.G. & McVicar, T.R. (2004) Determining Temporal Windows for Crop Discrimination with Remote Sensing: A Case Study in South-Eastern Australia. *Computers and Electronics in Agriculture*, **45**, 91-108.

Verstraete, M.M., Hutchinson, C.F., Grainger, A., Stafford Smith, M., Scholes, R.J., Reynolds, J.F., Barbosa, P., Léon, A. & Mbow, C. (2011) Towards a global drylands observing system: Observational requirements and institutional solutions. *Land Degradation & Development*, **22**, 198-213.

Woodcock, C.E., Allen, R., Anderson, M., Belward, A., Bindschadler, R., Cohen, W., Gao, F., Goward, S.N., Helder, D. & Helmer, E. (2008) Free Access to Landsat Imagery. *Science*, **320**, 1011a.

Wulder, M.A., White, J.C., Goward, S.N., Masek, J.G., Irons, J.R., Herold, M., Cohen, W.B., Loveland, T.R. & Woodcock, C.E. (2008) Landsat Continuity: Issues and Opportunities for Land Cover Monitoring. *Remote Sensing of Environment*, **112**, 955-969.

Zhu, Z. & Woodcock, C.E. (2012) Object-Based Cloud and Cloud Shadow Detection in Landsat Imagery. *Remote Sensing of Environment*, **118**, 83-94.

Zhu, Z. & Woodcock, C.E. (2014) Continuous Change Detection and Classification of Land Cover using all Available Landsat Data. Remote Sensing of Environment, 144, 152-171.

References [CrossRef]

Andres, L., Salas, W.A. & Skole, D. (1994) Fourier analysis of multi-temporal AVHRR data applied to a land cover classification. *Journal of Remote Sensing*, **115**, 1115-1121. CrossRef

Armston, J., Disney, M., Lewis, P.E., Scarth, P., Phinn, S., Lucas, R., Buntin, P. & Goodwin, N. (2013) Direct retrieval of canopy gap probability using airborne waveform lidar. *Remote Sensing of Environment*, **134**, 24-38. CrossRef

Cho, M.A., Mathieu, R., Asner, G.P., Naidoo, L., van Aardt, J., Ramoelo, A., Debba, P., Wessels, K., Main, R., Smit, I.P.J. & Erasmus, B. (2012) Mapping tree species composition in South African savannas using an integrated airborne spectral and LiDAR system. *Remote Sensing of Environment*, **125**, 214-226. CrossRef

Colgan, M.S., Baldeck, C.A., Féret, J.-B. & Asner, G.P. (2012) Mapping Savanna Tree Species at Ecosystem Scales Using Support Vector Machine Classification and BRDF Correction Airborne Hyperspectral and LiDAR Data. *Remote Sensing*, **4**, 3462-3480. CrossRef

Colomina, I. & Molina, P. (2104) Unmanned aerial systems for photogrammetry and remote sensing: A review. *ISPRS Journal of Photogrammetry and Remote Sensing*, **92**

Danaher, T., Scarth, P., Armston, J., Collett, L., Kitchen, J. & Gillingham, S. (2010) Remote Sensing of Tree-Grass Systems: The Eastern Australian Woodlands. *Ecosystem Function in Savannas: Measurement and Modeling at Landscape to Global Scales* (ed. by M.J. Hill and N.P. Hanan), pp. 175-194. CRC Press, Boca Raton, USA.

de Blécourt, M., Röder, A., Gröngröft, A., Baumann, S., Frantz, D. & Eschenbach, A. (2018) Deforestation for agricultural expansion in SW Zambia and NE Namibia and the impacts on soil fertility, and soil organic carbon and nutrient levels. *This Volume*,

DeFries, R., Achard, F., Brown, S., Herold, M., Murdiyarso, D., Schlamadinger, B. & de Souza, C. (2007) Earth observations for estimating greenhouse gas emissions from deforestation in developing countries. *Environmental Science & Policy*, **10**, 385-394. CrossRef

Flood, N., Danaher, T., Gill, T.K. & Gillingham, S.S. (2013) An Operational Scheme for Deriving Standardised Surface Reflectance from Landsat TM/ETM+ and SPOT HRG Imagery for Eastern Australia. *Remote Sensing*, **5**, 83-109. CrossRef

Frantz, D., Röder, A., Udelhoven, T. & Schmidt, M. (2015a) Enhancing the Detectability of Clouds and Their Shadows in Multitemporal Dryland Landsat Imagery: Extending Fmask. *IEEE Geoscience and Remote Sensing Letters*, **12**, 1242-1246. CrossRef

Frantz, D., Röder, A., Stellmes, M. & Hill, J. (2015c) On the Derivation of a Spatially Distributed Aerosol Climatology for its Incorporation in a Radiometric Landsat Preprocessing Framework. *Remote Sensing Letters*, **6**, 647-656. CrossRef

Frantz, D., Röder, A., Stellmes, M. & Hill, J. (2016a) An Operational Radiometric Landsat Preprocessing Framework for Large-Area Time Series Applications. *IEEE Transactions on Geoscience and Remote Sensing*, **54**, 3928-3943. CrossRef

Frantz, D., Stellmes, M., Röder, A. & Hill, J. (2016e) Fire spread from MODIS burned area data: obtaining fire dynamics information for every single fire. *International Journal of Wildland Fire*. CrossRef

Frantz, D., Röder, A., Stellmes, M. & Hill, J. (2017) Phenology-adaptive pixel-based compositing using optical earth observation imagery. *Remote Sensing of Environment*, **190**, 331-347. CrossRef

Frantz, D., Stellmes, M., Röder, A., Udelhoven, T., Mader, S. & Hill, J. (2016g) Improving the Spatial Resolution of Land Surface Phenology by Fusing Medium- and Coarse-Resolution Inputs. *IEEE Transactions on Geoscience and Remote Sensing*, **54**, 4153-4164. CrossRef

Gao, F., Masek, J., Schwaller, M. & Hall, F. (2006) On the Blending of the Landsat and MODIS Surface Reflectance: Predicting Daily Landsat Surface Reflectance. *IEEE Transactions on Geoscience and Remote Sensing*, **44**, 2207-2218. CrossRef

Graz, F.P. (2003) An HTML-based Concept Model of the Dry Savanna Woodland Ecosystem for Teaching and Learning. *Ecology & Society*, **7**, 9. CrossRef

Griffiths, P., Müller, D., Kuemmerle, T. & Hostert, P. (2013a) Agricultural Land Change in the Carpathian Ecoregion after the Breakdown of Socialism and Expansion of the European Union. *Environmental Research Letters*, **8.** CrossRef

Griffiths, P., van der Linden, S., Kuemmerle, T. & Hostert, P. (2013b) A Pixel-Based Landsat Compositing Algorithm for Large Area Land Cover Mapping. *IEEE Journal of Selected Topics in Applied Earth Observations and Remote Sensing*, **6**, 2088-2101. CrossRef

Hansen, M.C., Potapov, P.V., Moore, R., Hancher, M., Turubanova, S.A., Tyukavina, A., Thau, D., Stehman, S.V., Goetz, S.J., Loveland, T.R., Kommareddy, A., Egorov, A., Chini, L., Justice, C.O. & Townshend, J.R.G. (2013) High-Resolution Global Maps of 21st-Century Forest Cover Change. *Science*, **342**, 850-853. CrossRef

Herold, M., Roman-Cuesta, R.M., Mollicone, D., Hirata, Y., Van Laake, P., Asner, G.P., Souza, C., Skutsch, M., Avitabile, V. & MacDicken, K. (2011a) Options for monitoring and estimating historical carbon emissions from forest degradation in the context of REDD#. *Carbon Balance and Management*, **6**, 1-7. CrossRef

Herold, M., Román-Cuesta, R.M., Mollicone, D., Hirata, Y., Van Laake, P., Asner, G.P., Souza, C., Skutsch, M., Avitabile, V. & MacDicken, K. (2011b) Options for Monitoring and Estimating Historical Carbon Emissions from Forest Degradation in the Context of REDD+. *Carbon Balance and Management*, **6**, 1-7. CrossRef

Huete, A., Justice, C.O. & Van Leeuwen, W. (1999) MODIS vegetation index (MOD13). *Algorithm theoretical basis document*, **3.**

Jonsson, P. & Eklundh, L. (2002) Seasonality Extraction by Function Fitting to Time-Series of Satellite Sensor Data. *IEEE Transactions on Geoscience and Remote Sensing*, **40**, 1824-1832. CrossRef

Joshi, N., Baumann, M., Ehammer, A., Fensholt, R., Grogan, K., Hostert, P., Jepsen, M.R., Kuemmerle, T., Meyfroidt, P., Mitchard, E.T.A., Reiche, J., Ryan, C.M. & Waske, B. (2016) A Review of the Application of Optical and Radar Remote Sensing Data Fusion to Land Use Mapping and Monitoring. *Remote Sensing*, **8**, 1-23. CrossRef

Keeley, J.E. (2009) Fire intensity, fire severity and burn severity: a brief review and suggested usage. *International Journal of Wildland Fire*, **18**, 116-126. CrossRef

Kennedy, R.E., Yang, Z. & Cohen, W.B. (2010) Detecting Trends in Forest Disturbance and Recovery using Yearly Landsat Time Series: 1. LandTrendr — Temporal Segmentation Algorithms. *Remote Sensing of Environment*, **114**, 2897-2910. CrossRef

Lefsky, M.A., Cohen, W.B., Parker, G., G. & Harding, D.J. (2002) Lidar Remote Sensing for Ecosystem Studies. *BioScience*, **52**, 19-30. CrossRef

Lucas, R., Cronin, N., Lee, A., Moghaddam, M., Witte, C. & Tickle, P. (2006) Empirical relationships between AIRSAR backscatter and LiDAR-derived forest biomass, Queensland, Australia. *Remote Sensing of Environment*, **100**, 407-425. CrossRef

Lucas, R., Lee, A., Armston, J., Carreiras, J.M.B., Viergever, K.M., Bunting, P., Clewley, D., Moghaddam, M., Siqueira, P. & Woodhouse, I. (2011) Quantifying Carbon in Savannas: The Role of Active Sensors in Measurements of Tree Structure and Biomass. *Ecosystem Function in Savannas: Measurement and Modelling at Landscape to Global Scales* (ed. by M.J. Hill and N.P. Hanan), pp. 155-174. CRC Press, Boca Raton, London, New York.

Mader, S. (2012) *A Framework for the Phenological Analysis of Hypertemporal Remote Sensing Data Based on Polynomial Spline Models*. Ph.D. dissertation, Trier University, Trier, Germany.

Naidoo, L., Cho, M.A., Mathieu, R. & Asner, G.P. (2012) Classification of savanna tree species, in the Greater Kruger National Park region, by integrating hyperspectral and LiDAR data in a Random Forest data mining environment. *ISPRS Journal of Photogrammetry and Remote Sensing*, **69**, 167-179. CrossRef

Oldeland, J., Große-Stoltenberg, A., Naftal, L. & Strohbach, B.J. (2017) The Potential of UAV Derived Image Features for Discriminating Savannah Tree Species. *The Roles of Remote Sensing in Nature Conservation. A Practical Guide and Case Studies.* (ed. by R. Diaz-Delgado, R. Lucas and C. Hurford), pp. 183-202. Springer, London, New York.

Oldeland, J., Dorigo, W., Lieckfeld, L., Lucieer, A. & Jürgens, N. (2010) Combining vegetation indices, constrained ordination and fuzzy classification for mapping semi-natural vegetation units from hyperspectral imager. *Remote Sensing of Environment*, **114**, 1155-1166. CrossRef

Parduhn, D. & Frantz, D. (2018) "This is not Deforestation". Seeing deforestation in Zambia from afar and nearby. *This Volume*,

Reiche, J., Verbesselt, J., Hoekman, D. & Herold, M. (2015) Fusing Landsat and SAR time series to detect deforestation in the tropics. *Remote Sensing of Environment*, **156**, 276-293. CrossRef

Revermann, R., Finckh, M., Stellmes, M., Strohbach, B., Frantz, D. & Oldeland, J. (2016) Linking land surface phenology and vegetation-plot databases to model terrestrial plant alpha diversity of the Okavango Basin. *Remote Sensing*, **8**, 470. CrossRef

Röder, A., Udelhoven, T., Hill, J., del Barrio, G. & Tsiourlis, G. (2008) Trend Analysis of Landsat-TM and -ETM+ Imagery to Monitor Grazing Impact in a Rangeland Ecosystem in Northern Greece. *Remote Sensing of Environment*, **112**, 2863-2875. CrossRef

Röder, A., Pröpper, M., Stellmes, M., Schneibel, A. & Hill, J. (2015) Assessing urban growth and rural land use transformations in a cross-border situation in Northern Namibia and Southern Angola. *Land Use Policy*, **42**, 340-354. CrossRef

Roy, D.P., Zhang, H.K., Ju, J., Gomez-Dans, J.L., Lewis, P.E., Schaaf, C.B., Sun, Q., Li, J., Huang, H. & Kovalskyy, V. (2016) A General Method to Normalize Landsat Reflectance Data to Nadir BRDF Adjusted Reflectance. *Remote Sensing of Environment*, **176**, 255-271. CrossRef

Schneibel, A., Röder, A., Stellmes, M. & Frantz, D. (2018) Long-term lan use change analysis in south-central Angola. Assessing the trade-off between major ecosystem services with remote sensing data. This Volume. CrossRef

Schneibel, A., Stellmes, M., Röder, A., Finckh, M., Revermann, R., Frantz, D. & Hill, J. (2016) Evaluating the trade-off between food and timber resulting from the conversion of Miombo forests to agricultural land in Angola using multi-temporal Landsat data. *Science of the Total Environment*, **548**, 390-401. CrossRef

Scholes, R.J., Mace, G.M., Turner, W., Geller, G.N., Jürgens, N., Larigauderie, A., Muchoney, D., Walther, B.A. & Mooney, H.A. (2008) Toward a Global Biodiversity Observing System. *Science*, **321**, 1044-1045. CrossRef

Stefanski, J., Kuemmerle, T., Chaskovskyy, O., Griffiths, P., Havryluk, V., Knorn, J., Korol, N., Sieber, A. & Waske, B. (2014) Mapping Land Management Regimes in Western Ukraine Using Optical and SAR Data. *Remote Sensing*, **6**, 5279-5305. CrossRef

Stellmes, M., Frantz, D., Finckh, M. & Revermann, R. (2013a) Okavango Basin - Earth Observation. *Environmental Assessments in the Okavango region* (ed. by J. Oldeland, C. Erb, M. Finckh and N. Jürgens), pp. 23-27. CrossRef

Stellmes, M., Röder, A., Udelhoven, T. & Hill, J. (2013b) Mapping Syndromes of Land Change in Spain with Remote Sensing Time Series, Demographic and Climatic Data. *Land Use Policy*, **30**, 685-702. CrossRef

Stellmes, M., Frantz, D., Finckh, M., Revermann, R., Röder, A. & Hill, J. (2013e) Fire frequency, fire seasonality and fire intensity within the Okavango region derived from MODIS fire products. *Biodiversity & Ecology*, **5**, 351-362. CrossRef

Stoffels, J., Hill, J., Sachtleber, T., Mader, S., Buddenbaum, H., Stern, O., Langshausen, J., Dietz, J. & Ontrup, G. (2015) Satellite-Based Derivation of High-Resolution Forest Information Layers for Operational Forest Management. *Forests*, **6**, 1982-2013. CrossRef

Tanré, D., Deroo, C., Duhaut, P., Herman, M., Morcrette, J.J., Perbos, J. & Deschamps, P.Y. (1990) Description of a Computer Code to Simulate the Satellite Signal in the Solar Spectrum: The 5S Code. *International Journal of Remote Sensing*, **11**, 659-668. CrossRef

Udelhoven, T., Stellmes, M. & Röder, A. (2015) Assessing rainfall-EVI relationships in the Okavango catchment employing MODIS time series data and distributed lag models. *Remote Sensing Time Series. Revealing Land Surface Dynamics* (ed. by C. Kuenzer, S. Dech and S. Wagner), pp. 225-245. Springer, Berlin, Heidelberg.

Van Niel, T.G. & McVicar, T.R. (2004) Determining Temporal Windows for Crop Discrimination with Remote Sensing: A Case Study in South-Eastern Australia. *Computers and Electronics in Agriculture*, **45**, 91-108. CrossRef

Verstraete, M.M., Hutchinson, C.F., Grainger, A., Stafford Smith, M., Scholes, R.J., Reynolds, J.F., Barbosa, P., Léon, A. & Mbow, C. (2011) Towards a global drylands observing system: Observational requirements and institutional solutions. *Land Degradation & Development*, **22**, 198-213. CrossRef

Woodcock, C.E., Allen, R., Anderson, M., Belward, A., Bindschadler, R., Cohen, W., Gao, F., Goward, S.N., Helder, D. & Helmer, E. (2008) Free Access to Landsat Imagery. *Science*, **320**, 1011a. CrossRef

Wulder, M.A., White, J.C., Goward, S.N., Masek, J.G., Irons, J.R., Herold, M., Cohen, W.B., Loveland, T.R. & Woodcock, C.E. (2008) Landsat Continuity: Issues and Opportunities for Land Cover Monitoring. *Remote Sensing of Environment*, **112**, 955-969. CrossRef

Zhu, Z. & Woodcock, C.E. (2012) Object-Based Cloud and Cloud Shadow Detection in Landsat Imagery. *Remote Sensing of Environment*, **118**, 83-94. CrossRef

Zhu, Z. & Woodcock, C.E. (2014) Continuous Change Detection and Classification of Land Cover using all Available Landsat Data. *Remote Sensing of Environment*, **144**, 152-171. CrossRef